A Subarray Manifold Revealing Projection for Partially Blind Identification and Beamforming

Sofiène Affes, Saeed Gazor, and Yves Grenier, *Member, IEEE*

***Abstract*—We consider the problem of locating and extracting sources received by an array of sensors in two significant cases. In one case, sensor positions are partially unknown. In the other one, the propagation to a subset of sensors is unknown. The core of the algorithm is partially blind identification of steering vectors. It relies on a tracking procedure with low computational complexity. We apply it to the calibration of maneuvering and towed arrays receiving multiple and correlated sources.**

I. Introduction and Formulation

In array processing, the use of a higher number of array sensors when available has well-established advantages. Indeed, performances improve in either beamforming, localization, or tracking. With towed and maneuvering arrays, some sensors are, however, unlocated. Hence, their inputs are usually unexploitable by these techniques. This shortcoming is actually observed in a larger situation where propagation to some "remote" sensors is different and unknown (e.g., due to multipath). We first show in this general case how to identify propagation vectors to these sensors. We then explain how to reveal their positions in the particular case of towed and maneuvering arrays.

Classical source localization methods are indeed very sensitive to calibration errors, and usually require fully located uniform linear arrays. To extend their application to distorted arrays, previous contributions [1], [2] introduced interpolation techniques to design a virtual array with any desired shape. However, these techniques require all actual sensor locations. Recently, other methods [3], [4] extended the application of source localization to partially calibrated arrays. Without explicit identification of unlocated sensor positions, Stoica *et al.* derived in [4] an instrumental variable method for DOA estimation that is robust to calibration errors. For full array-shape calibration, Marcos applied a linear operator called the "propagator" to provide rough estimates of unlocated sensor locations [3].

Manuscript received October 13, 1995. The associate editor coordinating the review of this letter and approving it for publication was Prof. T. S. Durrani.

The authors are with the Ecole Nationale Supérieure des Télécommunications, Département Signal, 75634 Paris Cedex 13, France (e-mail: affes@sig.enst.fr).

S. Affes is currently with INRS-Télécom., Montreal, Canada (e-mail: affes@inrs-telecom.uquebec.ca).

Publisher Item Identifier S 1070-9908(96)04971-1.

Contrary to these methods, we explicitly identify propagation vectors to unlocated sensors and reveal their exact positions in the case of towed and maneuvering arrays at a lower order of complexity. Recently, we proposed in [5] and [6] a source-subspace-based procedure for tracking steering vectors in the array manifold. In this contribution, we restrict the projection of steering vectors in [5] and [6] to the subarray manifold of exploitable sensors in a partially blind scheme. We show that the resulting algorithm fully identifies steering vectors, and we confirm by simulations its high performance in coherent source extraction and tracking.

At time t, we consider p sources $s_{k,t}$ at distinct locations $\theta^s_{k,t}$ for $k = 1, \ldots, p$, received by an array of m sensors at different positions $\theta^a_{i,t}$ for $i = 1, \ldots, m$. We assume that $p \leq m$. The vector of observation signals say X_t is corrupted by an additive noise vector N_t as follows:

$$X_t = G_t S_t + N_t = \begin{bmatrix} U_t \\ V_t \end{bmatrix} S_t + N_t \tag{1}$$

where the signal vector is $S_t = [s_{1,t}, \cdots, s_{p,t}]^T$, and where $G_t = [G_{1,t}, \cdots, G_{p,t}]$ is the $m \times p$ steering matrix. The $\bar{m} \times p$ submatrix U_t corresponds to a defined and known propagation model F to the subarray of the first $\bar{m} \geq p$ sensors. It is defined such that each column vector $U_{k,t} = F(\theta^s_{k,t}, \theta^a_{1,t}, \ldots, \theta^a_{\bar{m},t})$ be in the subarray manifold say $\mathcal{G}_{\bar{m}}$ for $k = 1, \ldots, p$. In the case of a far-field propagation in a 2-D space, we can write the modeling function F as follows:

$$\begin{aligned} U_{k,t} &= F(\theta^s_{k,t}, \theta^a_{1,t}, \ldots, \theta^a_{\bar{m},t}) \\ &= \left[e^{-j\frac{2\pi}{\lambda}\theta^{a\,T}_{1,t}\theta^s_{k,t}}, \ldots, e^{-j\frac{2\pi}{\lambda}\theta^{a\,T}_{\bar{m},t}\theta^s_{k,t}}\right]^T \end{aligned} \tag{2}$$

where $\theta^s_{k,t} = [\frac{2\pi}{\lambda}\sin(\phi_{k,t}), \frac{2\pi}{\lambda}\cos(\phi_{k,t})]^T$ is the wave-vector of the kth source, and where $\theta^a_{i,t} = [x_{i,t}, y_{i,t}]^T$ is the ith sensor coordinates vector. $\phi_{k,t}$ is the DOA of the kth source and λ is the wave-length. We assume that F involves no ambiguity in $\mathcal{G}_{\bar{m}}$. On the other hand, the $(m - \bar{m}) \times p$ submatrix V_t is an unknown steering matrix which denotes the blind part of propagation. To avoid ambiguities due to any multiplicative factor between G_t and S_t, we fix $\|G_{k,t}\|^2 = \|U_{k,t}\|^2 + \|V_{k,t}\|^2 = m$. We finally assume that initial locations $\theta^s_{1,0}, \ldots, \theta^s_{p,0}$ and $\theta^a_{1,0}, \ldots, \theta^a_{\bar{m},0}$ are respectively approximated by $\hat{\theta}^s_{1,0}, \ldots, \hat{\theta}^s_{p,0}$ and $\hat{\theta}^a_{1,0}, \ldots, \hat{\theta}^a_{\bar{m},0}$. These rough initial estimates can be *a priori* given or computed by a robust localization method as made in [3] and [4].

II. Proposed Algorithm

We implement the algorithm in three steps:

A. Partially Blind Beamforming

We assume that an estimate of G_t say $\hat{G}_t$ is available. Actually, $\hat{U}_0$ is given by the initial values $\hat{\theta}^s_{k,0}$ and $\hat{\theta}^a_{i,0}$, whereas $\hat{V}_t$ is started at random and denotes the blind part of beamforming. We estimate the signal vector S_t with a $m \times p$ beamforming matrix W_t by

$$\hat{S}_t = W_t^H X_t \tag{3}$$

such that the kth column beamformer of W_t for $k = 1, \ldots, p$ be distortionless to the kth source and provide null constraints to the others (i.e., $W_t^H \hat{G}_t = I_p$). We can apply $W_t = \hat{G}_t(\hat{G}_t^H \hat{G}_t)^{-1}$, which is optimal for white and uncorrelated noise reduction as reported in [5] and [6], with an order of complexity of $O(mp^2 + mp + p^3 + p^2)$ operations. In the presence of other unknown sources and colored noise, we may apply an optimal multidimensional GSC structure including the constraint $W_t^H \hat{G}_t = I_p$ (see the authors' references in [5] and [6]).

B. Partially Blind Identification of Steering Vectors

From the observation vector X_t and the estimated signal vector $\hat{S}_t$ given by $W_t = \hat{G}_t(\hat{G}_t^H \hat{G}_t)^{-1}$, we track G_t as in [5] and [6] by the following gradient-based tracking procedure

$$\begin{aligned}\tilde{G}_{t+1} = \begin{bmatrix} \tilde{U}_{t+1} \\ \tilde{V}_{t+1} \end{bmatrix} &= \hat{G}_t + \mu(X_t - \hat{G}_t \hat{S}_t)\hat{S}_t^H \\ &= \hat{G}_t + \mu(I_m - \hat{G}_t W_t^H) X_t X_t^H W_t \end{aligned} \tag{4}$$

where μ is an adaptation step-size. This estimate of G_{t+1}, which requires an order of $O(mp)$ operations is denoted at present by $\tilde{G}_{t+1}$ since $\tilde{U}_{t+1}$ is not necessarily in $\mathcal{G}_{\bar{m}}$.

To obtain $\hat{U}_{t+1}$ or, equivalently, $\hat{G}_{t+1}$, we assign $\tilde{U}_{t+1}$ in $\mathcal{G}_{\bar{m}}$ by structure fitting as in [5] and [6]. We first explicitly write the components of $\tilde{U}_{t+1} = [\tilde{\gamma}_{i,k,t+1} e^{-j\tilde{\varphi}_{i,k,t+1}}]$ and define its phase matrix by $\tilde{\Phi}_{t+1} = [\tilde{\varphi}_{i,k,t+1}]$. In the considered case of a far-field propagation in a 2-D space of (2), $\tilde{\varphi}_{i,k,t+1}$ should be approximated by $\hat{\varphi}_{i,k,t+1} = \hat{\theta}^{a^T}_{i,t+1} \hat{\theta}^s_{k,t+1}$, which denote the elements of $\hat{\Phi}_{t+1}$. This can be achieved by row-wise and column-wise linear regressions of $\tilde{\Phi}_{t+1}$ over, respectively, source and sensor positions. To avoid phase warping, we actually make these regressions over the phase matrix $\Delta\Phi_{t+1} = \tilde{\Phi}_{t+1} - \hat{\Phi}_t$ of $\tilde{G}_{t+1} - \hat{G}_t$ as explained in [5]. From the solutions $\hat{\theta}^s_{1,t+1}, \cdots, \hat{\theta}^s_{p,t+1}$ and $\hat{\theta}^a_{1,t+1}, \cdots, \hat{\theta}^a_{\bar{m},t+1}$ (see [5]), we reconstruct $\hat{U}_{k,t+1} = F(\hat{\theta}^s_{k,t+1}, \hat{\theta}^a_{1,t+1}, \ldots, \hat{\theta}^a_{\bar{m},t+1})$ and have $\hat{G}_{t+1} = [\hat{G}_{1,t+1}, \cdots, \hat{G}_{k,t+1}, \ldots, \hat{G}_{p,t+1}]$ where

$$\hat{G}_{k,t+1} = \begin{bmatrix} \hat{U}_{k,t+1} \\ \frac{\sqrt{m-\bar{m}}}{\|\tilde{V}_{k,t+1}\|} \tilde{V}_{k,t+1} \end{bmatrix} \quad \text{for } k = 1, \cdots, p. \tag{5}$$

This step requires an order of complexity of $O(mp)$ operations per sample [5], and a 3-D generalization or an application to the near-field case can be easily viewed with any array shape.

By analogy to [5] and [6], (4) derives from the minimization of the orthogonal projection to $\hat{G}_t$ of X_t by $E[\|(I_m - GW^H)X_t\|^2]$ subject to $W^H G = I_p$, and such that U be in the subarray manifold $\mathcal{G}_{\bar{m}}$. In [5] and [6], where all sensors are approximately located, we rather force G to be in $\mathcal{G}_m$. Without this bounding step, $\hat{G}_t$ converges in the source subspace to any linear combination of G_t when noise is spatially uncorrelated. On the other hand, simultaneous structure-fitting forces $\hat{G}_t$ to be also in the array-manifold regardless of noise structure (see the authors' references in [5] and [6]). Since the modeling function F in (2) is unambiguous, $\hat{G}_t$ necessarily converges to G_t in both the source subspace and the array manifold. Actually, any submatrix of at least any p rows of G_t is full rank when the corresponding subarray manifold is unambiguous, and still characterizes G_t in the source subspace in a unique manner when sources are not fully correlated (i.e., degenerate case). In particular, binding $\hat{U}_t$ in $\mathcal{G}_{\bar{m}}$ guarantees its convergence to U_t and forces convergence of both $\hat{G}_t$ to G_t and $\tilde{V}_t$ to V_t. This will be confirmed later by simulations.

At this point, we identify the blind part of propagation and address the first case where propagation to a subset of sensors is *a priori* unknown and arbitrary. Suppose now in a second case that propagation is *a priori* modeled but parameterized by unlocated sensor positions; then we can reveal the unknown subarray shape as shown below.

C. Localization of Unlocated Sensors

From estimated source positions and $\tilde{V}_t$, we want to reveal unlocated sensor positions. We consider here the case of a towed array where propagation to all sensors is identical to (2), but any unambiguous modeling function other than F can be viewed (e.g., near-field for located sensors and far-field for remote unlocated sensors). In a similar way, the phase matrix of $\tilde{V}_t$ denoted by $\tilde{\Psi}_t$ should be approximated by $\hat{\Psi}_t = [\hat{\theta}^{a^T}_{i,t} \hat{\theta}^s_{k,t}]$ the phase matrix of $\hat{V}_t$ for $i = \bar{m}+1, \ldots, m$ and $k = 1, \ldots, p$. However, rough estimates of sensor positions are required to remove the ambiguity due to phase warping of $\tilde{\Psi}_t$ elements within 2π.

In the considered case, towed arrays are fixed to flexible structures that bound the distance between two adjacent sensors (see Fig. 1(a)). Hence, any close location around $\hat{\theta}^a_{\bar{m},t+1}$, say, $\breve{\theta}^a_{\bar{m},t+1}$ is a good initialization of $\hat{\theta}^a_{\bar{m}+1,t+1}$ as soon as $\hat{G}_t$ converges to G_t. At that point, one iteration is usually sufficient to reveal $\theta^a_{\bar{m}+1,t+1}$ with reasonable precision. To recurrently reveal all unlocated sensor positions, we apply the following procedure for $i = \bar{m}+1, \ldots, m$

$$\hat{\theta}^a_{i,t+1} = \breve{\theta}^a_{i-1,t+1} + \hat{\Theta}^{s\#}_{t+1}(\tilde{\Psi}_{i,t+1} - \breve{\theta}^{a^T}_{i-1,t+1} \hat{\Theta}^s_{t+1})^T \tag{6}$$

where $\hat{\Theta}^{s\#}_{t+1} = (\hat{\Theta}^s_{t+1} \hat{\Theta}^{s^T}_{t+1})^{-1} \hat{\Theta}^s_{t+1}$ is the pseudoinverse of $\hat{\Theta}^s_{t+1} = [\hat{\theta}^s_{1,t+1}, \ldots, \hat{\theta}^s_{p,t+1}]$ and where $\tilde{\Psi}_{i,t+1}$ is the ith row of $\tilde{\Psi}_{t+1}$. We actually try a few positions of $\breve{\theta}^a_{i-1,t+1}$ uniformly distributed around $\hat{\theta}^a_{i-1,t+1}$ until $\tilde{\Psi}_{i,t+1}$ fits with $\hat{\theta}^{a^T}_{i,t+1} \hat{\Theta}^s_{t+1}$. As soon as we fully calibrate the array shape, we can apply structure-fitting of $\hat{G}_t$ in $\mathcal{G}_m$ and possibly track slow sensor motions as in [5] (i.e., $\breve{\theta}^a_{i-1,t+1} = \hat{\theta}^a_{i,t}$). This step requires an order of $O(mp)$ operations, whereas the global order of complexity of $O(mp^2 + mp + p^3 + p^2)$ is lower than required by [3] and [4].

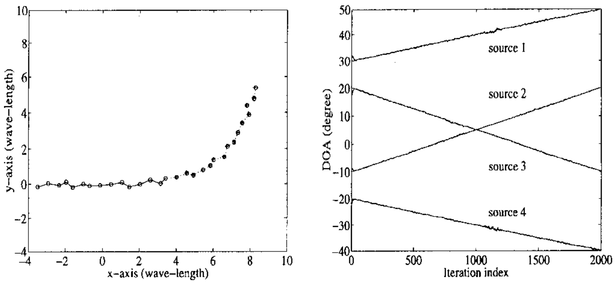

(a) (b)

Fig. 1. (a) Array geometry. Located subarray (solid line); unlocated subarray (dotted line); "o," true sensor positions; "+," estimated sensor positions. (b) DOA trajectories. True (dotted line); estimated (solid line).

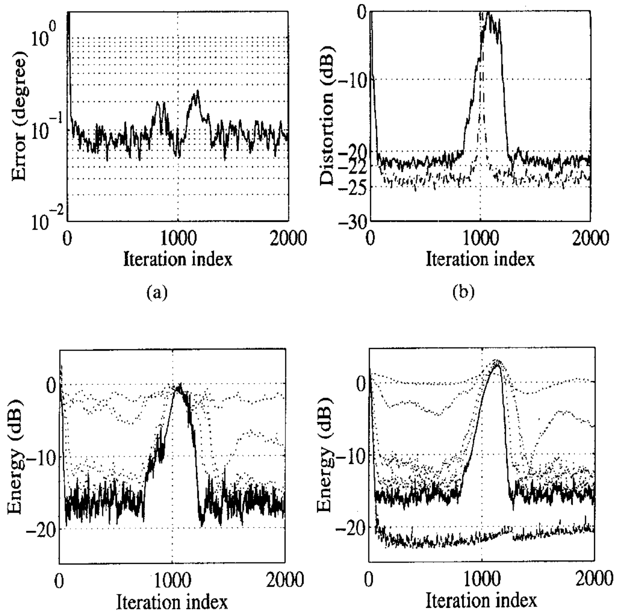

(a) (b)

(c) (d)

Fig. 2. (a) Absolute DOA error $E[\sum_{k=1}^{p} \frac{|\phi_{k,t}-\hat{\phi}_{k,t}|}{p}]$. (b) Distortion $E[\sum_{k=1}^{p} \frac{|s_{k,t}-\hat{s}_{k,t}|^2}{p}]$: Projection over $\mathcal{G}_{\bar{m}}$ (solid line); projection over $\mathcal{G}_m$ (dotted line). (c) Mean square error $E[\sum_{k=1}^{p} \frac{\|\hat{V}_{k,t}-\tilde{V}_{k,t}\|^2}{(m-\bar{m})p}] \nearrow$ with $\rho_c = 0$ (solid line); 0.5, 0.7, 0.9, 1 (dotted line). (d) Mean square error $E[\sum_{k=1}^{p} \frac{\|V_{k,t}-\hat{V}_{k,t}\|^2}{(m-\bar{m})p}] \nearrow$ with $\rho_c = 0$ (solid line); 0.5, 0.7, 0.9, 1 (dotted line); after projection over $\mathcal{G}_m$ ($\rho_c = 0$) (semidashed line).

III. Evaluation

We consider for simulations the configuration described in [4] of four mobile uncorrelated plane-wave sources with equal unit power [see Fig. 1(b)], corrupted here by uncorrelated white noise at a signal-to-noise ration (SNR) of 10 dB (see author's references in [5] and [6] for the case of colored noise). We also consider in Fig. 1(a) a towed array of 30 sensors with distortions similar to [3] and [4]. The first 15 sensor positions are given by [5] initially run with a uniform linear array of 15 sensors, which still approximates the located subarray in solid line with acceptable calibration errors.

The proposed algorithm exhibits in Fig. 1(b) a very good tracking behavior of mobile sources even during crossover. Details about the use of kinematics during crossovers are given in [6]. The algorithm self-corrects relatively high initial DOA errors. These errors are reduced to the range of 10^{-2} degree during tracking as shown in Fig. 2(a). However, residual noise without full projection of $\hat{G}_t$ over $\mathcal{G}_m$ is only of -SNR-$10\log_{10}(\bar{m}) \simeq -22$ dB (Fig. 2(b), solid line). This is the optimal performance in source extraction achievable with an array of $\bar{m}$ sensors. It is actually reached without any *a priori* knowledge of the propagation model to the remaining sensors. In Fig. 2(c), we plot in solid line structure-fitting errors given by (6). They perfectly reflect actual errors of partially blind identification plotted in solid line in Fig. 2(d). Notice that unlocated sensors are perfectly localized within 50 iterations when errors decrease below a given threshold. At that point, we plot in Fig. 1(a) the estimated sensor positions (dotted line). Calibration errors appear negligible when compared to [3]. We also switch structure-fitting to a full projection of $\hat{G}_t$ over $\mathcal{G}_m$. Now, this recovers the optimal performance of -SNR-$10\log_{10}(m) \simeq -25$ dB in residual noise achievable with an array of m sensors, and improves the behavior of source extraction during crossovers (Fig. 2(b), semidashed line). Notice that full structure-fitting improves identification errors plotted in the semidashed line in Fig. 2(d), but performance in source tracking, already high, is not noticeably enhanced.

We now evaluate the algorithm in the presence of correlated sources (not considered in [3] and [4]). We introduce an identical correlation factor between s_1 and s_2, and s_3 and s_4, successively fixed to $\rho_c = 0.5, 0.7, 0.9$ and 1. We notice that performance in source tracking (Fig. 1(b) and Fig. 2(a)) and source extraction prior to full structure-fitting (Fig. 2(b), solid line) remains unchanged even in the degenerate case where $\rho_c = 1$. On the other hand, identification and structure fitting deteriorate with increasing values of ρ_c as shown in dotted line in Fig. 2(c) and (d). For values beyond 0.7, degradation becomes severe and no longer permits localization of unlocated sensors. Below that range, we are still able to localize them and recover optimal performance in source extraction (Fig. 2(b), semidashed line).

References

[1] V. V. Krishna and A. Paulraj, "Direction-of-arrival estimation using eigenstructure methods for maneuvering arrays," *ICASSP'90*, Albuquerque, NM, Apr. 1990, vol. 5, pp. 2835–2838.

[2] B. Friedlander, "The root-MUSIC algorithm for direction finding with interpolated arrays," *Signal Processing*, vol. 30, no. 1, pp. 15–29, Jan. 1993.

[3] S. Marcos, "Calibration of a distorted array using a propagation operator," *JASA*, vol. 93, no. 4-1, pp. 1987–1994, Apr. 1993.

[4] P. Stoica, M. Cedervall, and T. Söderström, "Adaptive instrumental-variable method for robust direction-of-arrival estimation," *IEE Proc. Radar, Sonar Navig.*, vol. 142, no. 2, pp. 45–53, Apr. 1995.

[5] S. Gazor, S. Affes, and Y. Grenier, "Wideband multi-source beamforming with adaptive array location calibration and direction finding," *ICASSP'95*, Detroit, MI, May 1995, vol. III, pp. 1904–1907.

[6] S. Affes, S. Gazor, and Y. Grenier, "An algorithm for multi-source beamforming and multi-target tracking," *IEEE Trans. Signal Processing*, to appear June 1996.